Slow crack growth : models and experiments

Stéphane Santucci, Loïc Vanel, Sergio Ciliberto

Slow crack growth: models and experiments

S. Santucci, L. Vanel, S. Ciliberto
Laboratoire de Physique, CNRS UMR 5672,
Ecole Normale Supérieure de Lyon
46 allée d'Italie, 69364 Lyon Cedex 07, France

March 28, 2007

Abstract

The properties of slow crack growth in brittle materials are analyzed both theoretically and experimentally. We propose a model based on a thermally activated rupture process. Considering a 2D spring network submitted to an external load and to thermal noise, we show that a preexisting crack in the network may slowly grow because of stress fluctuations. An analytical solution is found for the evolution of the crack length as a function of time, the time to rupture and the statistics of the crack jumps. These theoretical predictions are verified by studying experimentally the subcritical growth of a single crack in thin sheets of paper. A good agreement between the theoretical predictions and the experimental results is found. In particular, our model suggests that the statistical stress fluctuations trigger rupture events at a nanometric scale corresponding to the diameter of cellulose microfibrils.

1 Introduction

Research on fracture has received a lot of attention from the physics community. This interest is obviously motivated by the numerous practical benefits that a better understanding of the fracturing processes in solid materials would bring to many engineering domains. But also from a theoretical point of view, the study of damaging processes in heterogeneous materials appears crucial in different fields of physics, and brings forward many challenging questions in particular in statistical physics [1, 2].

Here, we are interested in slow rupture processes observed when a material is submitted to a constant load below a critical rupture threshold (creep test). It is well known that the delay time (or lifetime) of the material before complete macroscopic rupture strongly depends on the applied stress. Thermodynamics has slowly emerged as a possible framework to describe delayed rupture of materials since early experiments have shown temperature dependence of lifetime with an Arrhenius law [3, 4]. The current understanding is that subcritical rupture can be thermally activated with an activation energy which depends on the applied stress. For elastic materials, several statistical models have been recently proposed in order to predict the lifetime [5, 6, 7, 8, 9, 10] and the average dynamics of a slowly growing crack [11]. In these models, it is assumed that the thermal noise inside the material induce stress fluctuations that will nucleate small cracks if the stress becomes larger than the local rupture threshold of the material. These models are interesting because in certain conditions they allow the prediction of the lifetime of a sample as a function of the macroscopic applied stress. However the test

of this idea is not simple because other models based on viscoelastic retardation of the crack formation [12, 13, 14] may in some cases explain the formation of the delayed crack.

The purpose of this paper is to review a series of experiments and theoretical studies that have been performed in order to test in some details the activation models in brittle materials, that is for materials whose stress-strain curve remains elastic till failure. Since the model we have chosen is a two dimensional one, the experiments are also performed in a situation very close to a 2D geometry. Specifically we have studied the slow propagation of a single crack in a thin sheet of paper which in dried atmosphere is a brittle material. As we will see, this geometry allows an accurate comparison with the theoretical predictions.

The paper is organized as follows: in section 2, we review the main properties of the model and we summarize the main predictions; in section 3, we describe the experimental apparatus and the properties of the averaged crack growth; in section 4, the statistics of the crack jumps is discussed. We conclude in section 5.

2 A model for the slow crack growth

It is very well known that when a material is submitted to a constant stress (creep test) it breaks after a certain time τ which is a function of the applied stress. We are interested in modeling this phenomenon for brittle materials. Specifically, we want to derive the dependence of the lifetime τ on the applied stress and of the damage, i.e. the number of broken bonds, as a function of time. A common approach to describe the creep rupture of materials is to introduce a time-dependent creep compliance or a rate of rupture which is a power law of the applied stress [15]. Instead of assuming a phenomenological law for the creep behavior, we use a statistical approach which takes into account the fact that at equilibrium there are always statistical fluctuations of stress with a variance which depends on the actual temperature of the material. These local stress fluctuations may be larger than the local rupture stress of the material, thus producing local damage.

2.1 A thermally activated crack nucleation

The starting point is the Griffith theory for fracture in a brittle material[16, 17]. Griffith's prediction of a critical crack size beyond which there is rupture, i.e. irreversible and fast crack growth, is derived from a potential energy taking into account the elastic energy due to the applied stress σ and the surface energy γ needed to open a crack as a function of a unique order parameter, the crack length L [1]. For a bidimensional geometry consisting of a flat sheet with a crack perpendicular to the direction of stress, the potential energy per unit thickness of the sheet reads:

$$E_G(L) = -\frac{\pi L^2 \sigma^2}{4Y} + 2\gamma L + E_0 \tag{1}$$

where Y is the Young modulus and E_0 is the elastic energy in the absence of crack. A typical example of the Griffith potential as a function of L is shown on fig.1. This potential energy reaches a maximum for the Griffith length $L_G = 4Y\gamma/(\pi\ \sigma^2)$ which in this case coincide with a critical length L_c beyond which no stable state exists except the separation of the solid in two broken pieces. Thus, a stressed solid without a crack appears to be in a metastable state as long as no crack with a critical length nucleates[5, 6].

Several authors [3, 4, 5, 6, 7] have used models essentially inspired by Griffith's energy concept and considered that the nucleation of a crack with critcal size could be thermally

[1] see [7] for a generalization of this approach taking into account crack opening.

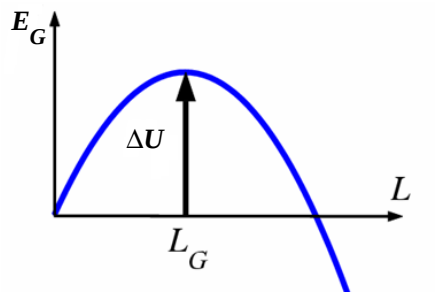

Figure 1: Sketch of the Griffith potential energy E_G as a function of crack length L.

activated. Then, the lifetime should follow an Arrhenius law:

$$\tau \sim \exp\left(\frac{\Delta U}{k_B T}\right) \tag{2}$$

where k_B is Boltzmann constant and T temperature. The energy barrier for the two-dimensional case can be obtained from eq.1 and scales as $\Delta U = E_G(L_G) \sim \sigma^{-2}$. Note that for a three-dimensional geometry the potential energy would give a barrier $\Delta U = E_G(L_G) \sim \sigma^{-4}$.

If this approach has permitted to reproduce and interpret qualitatively some experimental results[18, 19], quantitatively the temperature fluctuations appear too weak to be able to overcome the Griffith's energy barrier $\Delta U = E_G(L_G)$, except in the case of a Griffith length having atomic scale. Furthermore, there is another problem since this choice of energy barrier implicitly assumes that there is a possibility for the crack to explore reversible states of crack length between the initial and the critical one. If such a process could occur when the Griffith length is at atomic scale, this is certainly not true if one consider the experimental case where a preexisting macroscopic crack is growing progressively. In fact, this approach cannot describe any kind of dynamics where the rupture process appears to be irreversible.

2.2 An irreversible and thermally activated crack growth

In order to overcome the problem of irreversibility in thermally activated crack growth, let us start from a different point of view where irreversible rupture events can be caused by stress fluctuations due to thermal noise.

The uniaxial loading state of an homogeneous solid at fixed temperature is described by its free energy density: $\varphi(\sigma) = \sigma_m^2/2Y$, where σ_m is the internal stress of the material. Treating stress as a fluctuating internal variable in a fixed volume V, the probability to find a given stress is proportional to a Boltzmann factor $\exp(-\varphi V/k_B T)$. Expanding free energy about the equilibrium position σ_m, the distribution of stress σ_f is :

$$g(\sigma_f) \simeq \frac{1}{\sqrt{2\pi\langle\Delta\sigma\rangle^2}} \exp\left[-\frac{(\sigma_f - \sigma_m)^2}{2\langle\Delta\sigma\rangle^2}\right] \tag{3}$$

where $\langle\Delta\sigma\rangle^2 = k_B T/(V\partial^2\varphi/\partial\sigma^2) = k_B TY/V$[20]. When a crack is present, stress concentration increases the probability that breaking occurs at the crack tip rather than anywhere else. We assume that stress distribution at the crack tip remains the same as eq. (3) despite the

strong divergence of stress and the breakdown of linear elasticity. Since the stress intensity factor $K \approx \sigma\sqrt{L}$ gives a measure of stress intensity close to the crack tip for a crack with length L when the external load is σ, we choose to work directly with K and the stress at the crack tip is $\sigma_m = K/\sqrt{\lambda}$ where λ is a microscopic characteristic scale. Here we assume that the material is mainly elastic but at the scale λ it becomes discontinuous. For example in a perfect crystal, the only such scale would be the atomic scale, in a fibrous materials, like paper or fiber glass, we have an intermediate mesoscopic scale, i.e. the typical fiber size, and in the 2D elastic spring network the size of the elementary cell of the network. Within this description the threshold for rupture at the crack tip will be given by a critical value of stress intensity factor K_c as is usual laboratory practice.

In order to model crack rupture as a thermally activated process, we assume that a volume V of the material will break if the fluctuating stress K in this volume becomes larger than the threshold K_c. The breaking probability of the volume element is then:

$$P(K > K_c) = \int_{K_c}^{\infty} g(K)\lambda^{-1/2} dK = \int_{U_c}^{\infty} \frac{e^{-U_f} dU_f}{\sqrt{\pi U_f}} \tag{4}$$

where

$$U_f(K_f) = \frac{(K_f - K)^2 V}{2Y\ \lambda\ k_B T}, \qquad U_c = U_f(K_c) \qquad \text{and} \qquad K_f = \sigma_f\sqrt{\lambda}. \tag{5}$$

The lifetime of this volume element is [9]: $\tau_V = -\tau_e/\ln(1-P)$ where τ_e is an elementary time scale (typically, an inverse vibrational frequency). Then, the velocity v of the crack tip is simply $v = \lambda/\tau_V$. As long as $U_c \gg 1$ (in other words, when the energy barrier is larger than $k_B T$), we have $P \ll 1$, thus $\tau_V \simeq \tau_e/P$, $v \simeq \lambda P/\tau_e$ and we can approximate the integral in eq.(4) to get:

$$v = \frac{dL}{dt} \simeq \frac{\lambda}{\tau_e}\sqrt{\frac{Y\ \lambda\ k_B T}{2\pi V}}\frac{1}{K_c - K}\exp\left[-\frac{(K_c - K)^2\, V}{2\ Y\lambda\ k_B T}\right]. \tag{6}$$

Because K is a function of crack length L, eq.(6) is in fact a differential equation for the crack evolution. To solve this equation requires additional approximations since the dependence of stress intensity factor on crack length is non-linear. In numerical simulations of 2D networks of springs with thermal noise and in experiments one observes that all the relevant dynamics of the crack growth occurs for $L \simeq L_i$ and $L < L_c$. Then, the stress intensity factor can be written:

$$K \approx \sigma\sqrt{L} = \sigma\sqrt{L_i + (L - L_i)} \simeq K_i\left[1 + \frac{1}{2}(L - L_i)\right] \tag{7}$$

where the last equality is a reasonable approximation giving less than a 2% error on stress intensity factor as long as $L < 3/2L_i$. Another approximation will be to take $K = K_i$ in the pre-factor of the exponential, because neglecting the variation in stress intensity factor leads only to a logarithmic correction of the crack velocity. As a consequence of the last approximation, the crack velocity will tend to be underestimated.

Solution of the differential equation (6) is then :

$$t = \tau\left[1 - \exp\left(-\frac{L - L_i}{\zeta}\right)\right] \tag{8}$$

where τ gives the lifetime of the sample before fast rupture:

$$\tau = \tau_0 \exp\left[\frac{(K_c - K_i)^2 V}{2Y\lambda\ k_B T}\right] \qquad \text{with} \qquad \tau_0 = \frac{\tau_e}{\lambda}\ \frac{2\ \mathrm{L_i}}{\mathrm{K_i}}\ \sqrt{\frac{2\ \pi\ \mathrm{Y}\ \lambda\ \mathrm{k_B T}}{\mathrm{V}}} \tag{9}$$

and ζ is a characteristic growth length:

$$\zeta = \frac{2\ Y\ \lambda\ k_B T\ L_i}{V\ K_i(K_c - K_i)} \tag{10}$$

Note that the crack velocity : $\frac{dL}{dt} = \zeta/(\tau - t)$, diverges as time comes closer to lifetime τ, which simply means that when time τ is reached slow crack growth due to thermal activation is no longer the driving mechanism, and a crossover towards fast dynamic crack propagation will occur. The lifetime τ appearing in eq. (9) follows an Arrhenius law with an energy barrier

$$\Delta U = \left[\frac{(K_c - K_i)^2 V}{2Y\lambda}\right] \tag{11}$$

which is a function of initial and critical stress intensity factors. A similar scaling for the energy barrier was found by Marder [21].

2.3 Description of an intermittent dynamics and crack pinning

2.3.1 A modified Griffith energy barrier due to lattice trapping effect

The time evolution of the crack length predicted by eq.(8) has to be considered an average one. In reality both numerical simulations and experiments (see section 3) show that the crack tip progresses by jumps of various size and it can spend a lot of time in a fixed position. This dynamics can be understood by considering the existence of the characteristic microscopic scale λ introduced in the previous section. Indeed, the elastic description of a material at a discrete level leads to a lattice trapping effect [22] with an energy barrier which has been estimated analytically [21]. The other important effect of the discreteness is that L_c becomes larger than L_G. To get a physical picture of the trapping we may consider a 2D square lattice

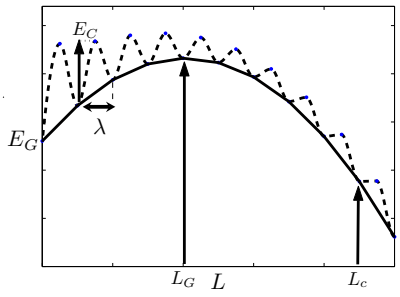

Figure 2: Sketch of the Griffith potential energy E_G as a function of crack length L with constant applied stress (solid line). The energy barriers E_C and the discretization scale λ are represented by the dashed curve.

of linear springs where the crack corresponds to a given number n of adjacent broken springs as described in [11]. The lattice is loaded with a constant stress σ and we estimate the minimum increase in potential energy needed to bring at the breaking threshold the spring at the tip of a crack of length $n\lambda$. This spring is submitted to a stress $\sigma_m = K/\sqrt{\lambda} = \sqrt{n}\ \sigma$. It is clear that in order to move the crack tip from the position n to $n+1$ the stress σ_f on the crack tip has to reach at least the material stress threshold for rupture σ_c. Thus to estimate the energy

barrier E_c that the system has to overcome to move the crack from n to $n+1$ we consider again the free energy density defined in sec. 2.2. The increase E_f of the free energy density produced by a an increase of the stress σ_f on the crack tip can be computed by a Taylor expansion of the bulk elastic free energy density around the equilibrium value of the stress σ_m, i.e. $E_f(\sigma_m) \simeq (\sigma_f - \sigma_m)^2/2Y$. As the crack moves only if $\sigma_f \geq \sigma_c$, the energy barrier that the system has to overcome is $E_c(\sigma_m) \simeq (\sigma_c - \sigma_m)^2/2Y$. To each position of the crack tip corresponds a different value of the energy barrier since σ_m,the stress at the tip, increases with the crack length. Once the spring breaks, the crack moves by at least one lattice spacing λ. The equilibrium potential energy of the whole system is given by the Griffith energy eq.(1). These simple arguments have been checked in a numerical simulation of the 2D spring lattice loaded with a constant stress. The energy barrier E_c is obtained by applying an external force on the spring at the crack tip and computing the change in elastic energy of the whole lattice and the work done by the constant force at the boundaries. The results of the simulation is plotted in Fig.2 where we represent the energy barrier of trapping schematically[2] (dashed line) and the Griffith energy (continuous line). In agreement with previous analysis [21], we find that the crack length L_c at which the energy barrier becomes zero is much larger than the Griffith length L_G where the equilibrium potential energy reaches its maximal value.

2.3.2 Irreversible thermally activated stepwise growth

We now recompute the mean crack speed v by considering the thermally activated and irreversible motion of a crack in the rugged potential energy landscape introduced above. Below L_c, the energy barriers $E_c(\sigma_m)$ trap the crack in a metastable state for an average time τ_p depending on the barrier height. Irreversible crack growth is a very reasonable assumption when $L > L_G$ since the decrease in equilibrium potential energy makes more likely for the crack to open than to close. As already mentioned in the previous section, when a fluctuation σ_f occurs, it will increase locally the free energy per unit volume by $E_f(\sigma_m) \simeq (\sigma_f - \sigma_m)^2/2Y$. The energy E_f can be used by the crack to overcome the barrier. If there are no dissipative mechanisms the crack will grow indefinitely when $L > L_G$ as the barriers get smaller and smaller and the release of elastic energy helps to reach a more energetically favorable position. We introduce a simple mechanism of crack arrest assuming that after overcoming the energy barrier the crack looses an energy identical to the barrier size and does not gain any momentum from the elastic release of energy (experimentally, dissipation will come from acoustic wave emissions, viscous or plastic flow, etc.). When the crack reaches the next trap it still has an energy $E_f - E_c$ which might be sufficient to overcome the next barrier. For a given fluctuation energy E_f, the crack will typically have enough energy to overcome a number of barriers $n = E_f(\sigma_m)/E_c(\sigma_m)$ and make a jump of size $s = n\lambda$ (the decrease of $E_c(\sigma_m)$ with σ_m during a jump of size s has been neglected). Thus s is related to the quantities defined in eq.(5), that is $s = U_f\ \lambda/U_c$. The probability distribution for E_f is explored at each elementary step τ_0, while the probability distribution of step size is explored after each average time τ_p spent in the trap. In order to relate the two probabilities, we express the mean velocity v in a different way as the ratio of the average step size to the average trapping time:

$$v = \frac{\int_\lambda^\infty sp(s)ds}{\tau_p} \tag{12}$$

where $p(s)$ is the distribution of the jump amplitudes at a given K. Identifying eq.(12) with $v = \lambda P/\tau_0$ (see paragraph 2.2 and eq.(4)) and using the above mentioned hypothesis that $s =$

[2]Note that the trapping barrier exists in fact for a fixed discrete length of the crack. The exact energy path that joins one equilibrium length to the next one is unknown

U_f λ/U_c we can write that $sp(s)ds = \exp(-U_f)\ (\pi U_f)^{-1/2}\ dU_f$. From the the normalization condition of the probability ($\int_\lambda^\infty p(s)ds = 1$), we obtain the probability distribution :

$$p(s) = N(U_c)\frac{\sqrt{\lambda}e^{-s/\xi}}{2s^{3/2}} \tag{13}$$

where $N(U_c) = \left[e^{-U_c} - \sqrt{\pi U_c}\mathrm{erfc}(\sqrt{\mathrm{U_c}})\right]^{-1}$ and $\xi = \lambda/U_c$. We find a power law with an exponent 3/2 and an exponential cut-off with a characteristic length $\xi \sim (K_c - K)^{-2}$ diverging at the critical stress K. Incidently, we note that this probability has a form similar to sub-critical point probability distributions in percolation theory [23]. From eq.(13), we can compute from this distribution the average and variance of step sizes:

$$\langle s\rangle = N(U_c)\frac{\lambda\sqrt{\pi}}{2\sqrt{U_c}}\mathrm{erfc}(\sqrt{\mathrm{U_c}}) \tag{14}$$

$$\langle s^2\rangle = N(U_c)\frac{\lambda^2\sqrt{\pi}}{4U_c^{3/2}}\left(\mathrm{erfc}(\sqrt{\mathrm{U_c}}) + 2\sqrt{\frac{\mathrm{U_c}}{\pi}}\mathrm{e}^{-\mathrm{U_c}}\right) \tag{15}$$

We obtain two asymptotical behaviors. When the relative energy barrier is high ($U_c \gg 1$), $\langle s\rangle \simeq \lambda$ and $\langle s^2\rangle \simeq \lambda^2$. In this limit, there is only one step size possible. When the relative energy barrier becomes low ($U_c \ll 1$), we predict a divergence at critical point : $\langle s\rangle \sim (K_c - K)^{-1}$ and $\langle s^2\rangle \sim (K_c - K)^{-3}$. Then, the crack velocity is expected to be dominated by the critical divergence of crack jumps.

3 The slow crack growth in a brittle material

The theoretical predictions of the previous section have been checked in an experiment in a quasi two dimensional geometry. Specifically, the samples are thin sheets of paper with an initial cut which are submitted to a constant applied stress [24, 25].

3.1 Experimental set-up

Crack growth is obtained by loading in mode 1 at a constant force F a sheet of fax paper (Alrey) with an initial crack in the center (fig. 3a). The sample dimensions are : height $h = 21$cm, width $w = 24$cm, and thickness $e = 50\mu$m.

The experimental set-up consists of a tensile machine driven by a motor (Micro Controle $UE42$) controlled electronically to move step by step (Micro Controle $ITL09$). The paper sheets are mounted on the tensile machine with both ends attached with glue tape and rolled twice over rigid bars clamped on jaws. The motor controls the displacement of one jaw (400 steps per micrometer) while the other jaw is rigidly fixed to a force gage (Hydrotonics-TC). The tensile machine is placed in a box with the humidity rate stabilized at 5%. In order to work on samples with the same initial crack shape and length L_i, we use calibrated razor blades mounted on a micrometric screw and we initiate a macroscopic crack precisely at the center of the sheet. The samples are loaded by increasing the distance between the jaws such that the resulting force F is perpendicular to the initial crack direction. A feedback loop allows us to adjust the displacement in order to keep the applied force F constant with a precision better than 0.5N and a response time less than 10ms. From the area A of a cross-section of the sheet, A being approximatively constant, we calculate the applied stress $\sigma = F/A$.

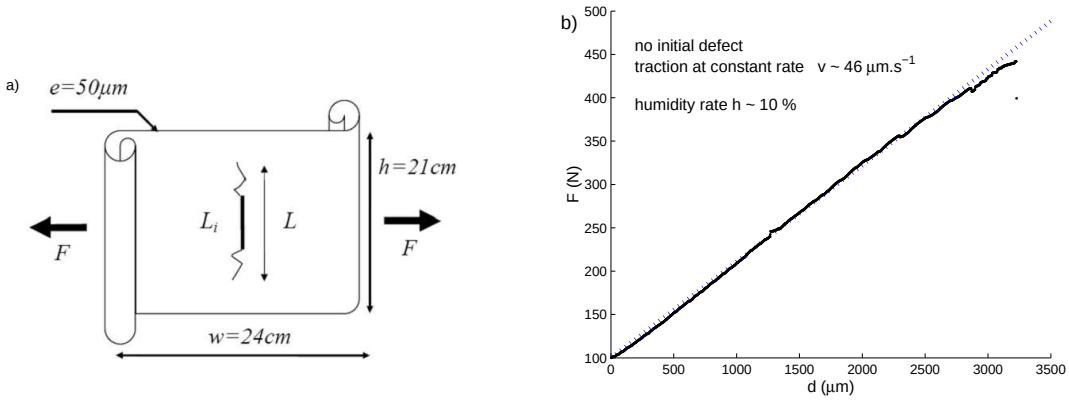

Figure 3: a) Sample geometry. b) Linear dependence between applied force and elongation until rupture.

3.1.1 Physical properties of paper

Sheets of fax paper in a dry atmosphere break in a brittle manner. This is evidenced by the elastic stress-strain dependence which is quasi-linear until rupture (fig. 3b). Another sign that rupture is essentially brittle is given by the very good match between the two opposite lips of the fracture surfaces observed on post-mortem samples. A sheet of paper is a complex

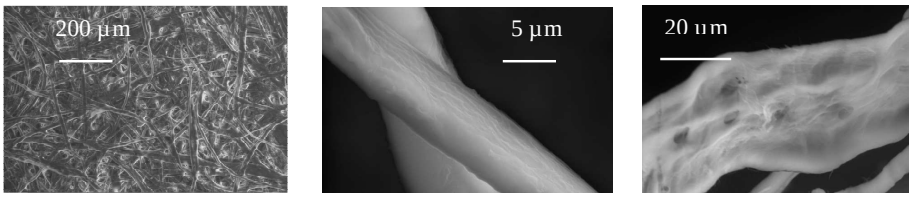

Figure 4: Scanning electron microscopy performed at GEMPPM (INSA Lyon) shows the microstructure of our samples and even the defects on the surface of a single fiber.

network of cellulose fibers. Scanning electron microscopy (see fig.4) on our samples shows fiber diameters between 4 and 50μm with an average of 18μm. Cellulose fibers are themselves a bundle of many microfibrils. Cellulose microfibrils have a cristalline structure (therefore, they are very brittle) and are consistently found to have a diameter $d = 2.5nm$ [27].

The mechanical properties of paper depend crucially on the humidity rate. To get reproducible results, the fax paper samples are kept at least one day at a low humidity rate ($< 10\%$) and during the experiment ($\simeq 5\%$). At constant humidity rate ($hu \simeq 5\%$) and room temperature, the Young modulus of the fax paper sheets is typically $Y = 3.3\,10^9 \mathrm{N.m}^{-2}$.

3.1.2 Direct observation and image analysis

We light the samples from the back. A high resolution and high speed digital camera (Photron Ultima 1024) collects the transmitted light and allows us to follow the crack growth. We

observe that the global deformation of the paper sheet during a creep experiment is correlated in a rather reproducible way to the crack growth whatever the rupture time. We use this property to trigger the camera at fixed increment of deformation (one micron) rather than at fixed increment in time. This avoids saturation of the onboard memory card when the crack growth is slow and makes the acquisition rate faster when the crack grows faster and starts to have an effect on global deformation. We acquire 2 frames at 250fps at each trigger and obtain around one thousand images per experiment. Image analysis is performed to extract

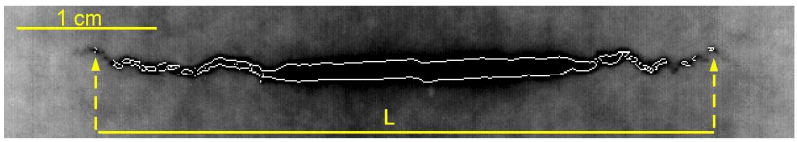

Figure 5: Extraction of the projected crack length L from the crack contour detected.

the length of the crack projected on the main direction of propagation, i.e. perpendicular to the direction of the applied load (fig. 5). Although the crack actually follows a sinuous trajectory, its projected length L gives the main contribution to the stress intensity factor K which we compute as: $K = \sigma\sqrt{\frac{\pi}{2}L\psi(\pi L/2H)}$, where $\psi(x) = \tan x/x$ is a correction due to the finite height H of the samples [17].

3.2 Experimental results

3.2.1 The single crack growth

For a given initial crack length L_i, subcritical crack growth is obtained by applying a constant force F so that $K(L_i)$ is smaller than a critical rupture threshold of the material K_c above which fast crack propagation would occur [24]. During an experiment, the crack length increases, and so does the stress intensity factor $K(L)$. This will cause the crack to accelerate until it reaches a critical length L_c for which $K(L_c) = K_c$.

On fig. 6a) we show a typical growth curve obtained during a creep experiment with an applied force $F = 270\,\mathrm{N}$ and an initial crack length $L_i = 1\mathrm{cm}$. Since time to rupture τ is a statistical quantity, we prefer to plot time evolution as a function of the crack length. We observe that the crack growth is actually intermittent. Essentially, there are periods of rest during which the crack tip is pinned and does not move, and other moments when the crack suddenly opens and advances of a certain step size s. The crack advances by jumps until it reaches a critical length L_c where the paper sheet breaks suddenly. On fig. 6 b) measurements of L_c are used to estimate the critical stress intensity factor $K_c = \sigma\sqrt{\pi L_c^{corr}/2}$, where we include the finite height corrections in the critical length L_c^{corr}. We find $K_c = 6\pm0.5\,\mathrm{MPa.m}^{1/2}$.

Beyond L_c, the crack runs across the whole sample (about 18cm in this case) in less than one second, with a crack speed $v > 300\mathrm{m.s}^{-1}$. For the same experimental conditions (same stress, same initial crack length, same temperature and same humidity rate), we observe a strong dispersion in growth curves and in lifetime while the critical length seems to be rather well defined. In order to characterize both the average crack growth and the stepwise growth dynamics, a statistical analysis is required. In this section we focus on the average dynamics (see also ref.[24]). The intermittent dynamics and in particular the step size statistics will be discussed in the next section (see also ref.[25]).

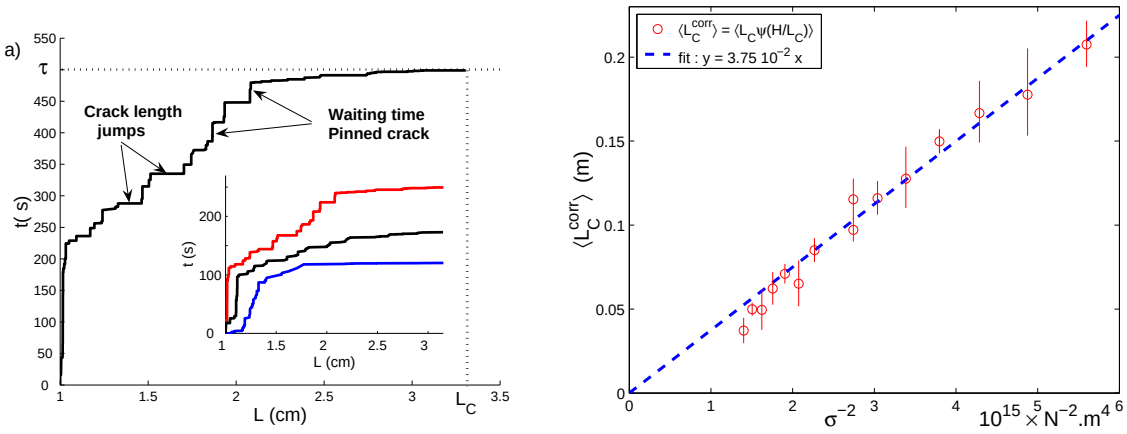

Figure 6: a) Typical stepwise growth curve for a creep experiment with an initial crack length $L_i = 1$cm submitted to a constant load $F = 270$N. The lifetime of the sample is $\tau = 500$s and the critical length $L_c = 3.3$cm. In insert, a strong dispersion is observed in crack growth profile and in lifetime for 3 creep experiments realized in the same conditions. b) Critical length of rupture L_c as function of the inverse square of the applied stress $1/\sigma^2$. The dashed line represents the best linear fit $y = K_c^2 x$. Its slope permits us to estimate the critical stress intensity factor K_c. Note that we introduce the finite height corrections in the critical length L_c^{corr}.

3.2.2 Statistically averaged crack growth

We have performed an extensive study of crack growth, varying the initial crack length from $L_i = 1$cm to $L_i = 4$cm and the applied force between $F = 140$N and $F = 280$N (corresponding to an initial stress intensity factor between $K_i = 2.7\text{MPa.m}^{1/2}$ and $K_i = 4.2\text{MPa.m}^{1/2}$) and repeating 5 to 20 experiments in the same conditions (stress, initial crack length, temperature and humidity rate). The resulting measured lifetime varied from a few seconds to a few days depending on the value of the applied stress or the temperature.

In order to characterize the average growth dynamics, we examine for given experimental conditions the average time $\langle t(L) \rangle$ the crack takes to reach a length L, where $< . >$ stands for ensemble average of $t(L)$ over many experiments. Even though the lifetime distribution is large and the growth dynamics intermittent, the average growth offers a regular behavior, very close to the exponential evolution given in eq.(8). Indeed, we obtain a very good fit of the data in fig. 7 with eq. (8) setting the mean lifetime to the experimentally measured value and using ζ as a unique free parameter. We note that the agreement is already quite good after averaging only 10 experiments in the same conditions.

Using the same procedure, we extract the characteristic growth length ζ for various experimental conditions. In the insert of fig. 7, rescaling the crack length by ζ and the time by τ for many different experimental conditions, we show that the data collapse on the functional form given by eq. (8). Moreover, we have checked that the deviation from the predicted average behavior reduces when increasing the number of experiments.

We now compare the measured ζ and τ with the theoretical predictions of paragraph 2. By setting the value of λ to the maximum fiber diameter that is $\lambda = 50\mu$m, we impose that there is no divergence of the stress in the fiber and that the maximum stress is controlled by the fiber size. Once λ is fixed, the only adjustable parameter is the activation volume

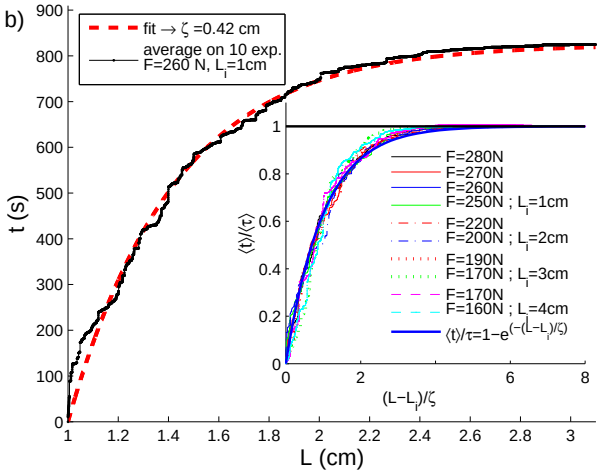

Figure 7: Statistical average of growth curves for 10 creep experiments realized in the same conditions ($L_i = 1$cm, $F = 270$N). The dashed line corresponds to a fit using equation eq. (8) with a single free parameter $\zeta = 0.41$cm. Insert: rescaled average time $\langle t \rangle / \tau$ as function of rescaled crack length $(L - L_i)/\zeta$ for various initial crack lengths and applied stress. The solid line corresponds to eq. (8).

V. In fig. 8a) we plot the measured values of ζ as a function of the theoretical one $\zeta_{th} V = 2Y\lambda k_B T L_i/[K_i(K_c - K_i)]$ (see eq.10). Using V as a free parameter, we find a characteristic scale $V^{1/3} = 1.5nm$ close to the microfibril diameter d. On fig. 8b, we show the value of ζ obtained by simulating the crack growth in a 2D square lattice of springs (see [11] for more details) and after averaging over more than 30 realizations of thermal noise. The agreement with the analytical model is very good in average, but there is still some dispersion due to the lack of statistics. We believe the same lack of statistics affects the experimental results in fig. 8a. Interestingly, the dispersion seems to increase with ζ both in the experiments and in the numerical simulation.

For a fixed value of applied force F and initial length L_i, varying temperature between 20°C and 120°C (symbols without error bar on fig. 8b) leads to variations of the rupture time up to four order of magnitude. In fig. 8b, we plot the rupture time as a function of $\Delta U/V k_B T = (K_c - K_i)^2/(2Y\ \lambda\ k_B T)$ as predicted by our model (see eqs.2,11). The temperature that enters in this relation is the actual themodynamic temperature, and not an effective temperature as in previous reports [26]. The error bars correspond to the experimental dispersion of measured rupture times. We see that there is a rather good collapse of the data whatever is the initial crack length L_i. Fixing the value of λ, from a fit of the data, we obtain independently a new estimate of V which gives a characteristic scale $V^{1/3} = 2.2nm$. Once again this estimate is close to the microfibril diameter d.

As a side remark, if we had considered rupture events were reversible, we could have as well considered that the energy barrier to overcome is given by the variation in Griffith potential energy between the length L_i and L_G: $\Delta E_G = E_G(L_G) - E_G(L_i)$. Given the material parameters of paper and the experimental conditions in which we observe rupture, this would have given us a typical value $\Delta E_G/k_B T \sim 10^{18}$ and rupture time virtually infinite. This

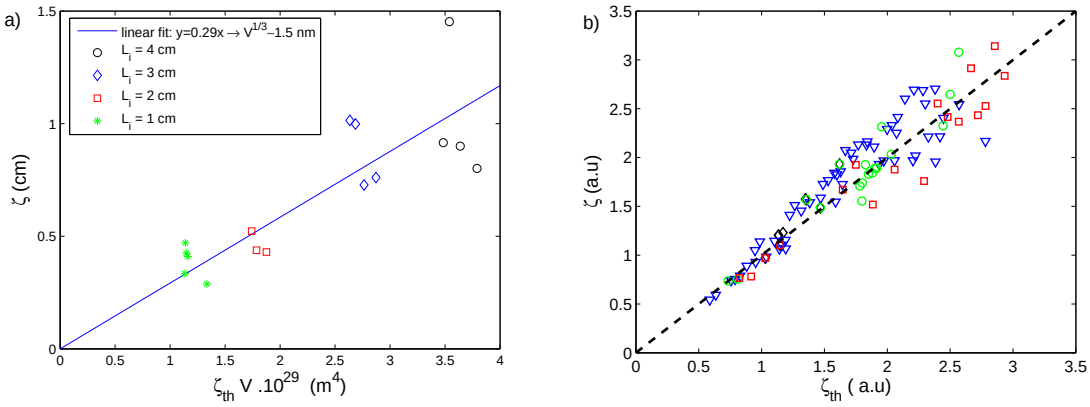

Figure 8: a) Experimental value of ζ extracted from the average growth profile as a function of the prediction of the thermally activated rupture model. The line represents the best linear fit $y = x/V$. Its slope permits us to obtain a characteristic length scale for rupture: $V^{1/3} \sim 1.5\,\mathrm{nm}$. b) ζ extracted from the average growth profile from numerical simulations [11] versus the predictions of our model of activated rupture. Each point corresponds to an average over 30 numerical experiments, at least. The solid line shows the behavior expected from the model (slope = 1).

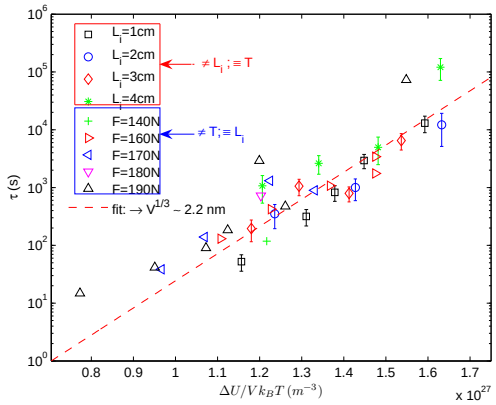

Figure 9: Logarithm of lifetimes as a function of the dimensional factor $\Delta U/(V k_B T)$ predicted by eq. 2 for different values of L_i, F and T. The slope of the best fit $\log \tau \propto \Delta U/k_B T$ (dashed line) gives an estimation of the characteristic length scale $V^{1/3} \sim 2.2\mathrm{nm}$. Data points without error bars correspond to non-averaged measurements obtained when varying temperature with $L_i = 2cm$ and various fixed values of F.

enormous value, obviously physically wrong, comes from ignoring the irreversible character of rupture events.

3.2.3 Comparison between the Griffith length L_G and the critical length of rupture L_C

We have observed on fig.6b) that the critical length L_c for which the paper sheet breaks suddenly, scales with the inverse square of the applied stress $1/\sigma^2$. Thus, L_c scales with σ as the Griffith length $L_G = 4Y\gamma/(\pi\ \sigma^2)$ does. In fact, we would normally expect that they are the same length [16]. However, the lattice trapping model presented in paragraph 2.3 predicts that L_c and L_G can be two different lengths. In order to clarify which conclusion is correct, we have designed a method to compute the Griffith length in our experiments. For that purpose, we need to estimate the surface energy γ needed to open a crack. Assuming

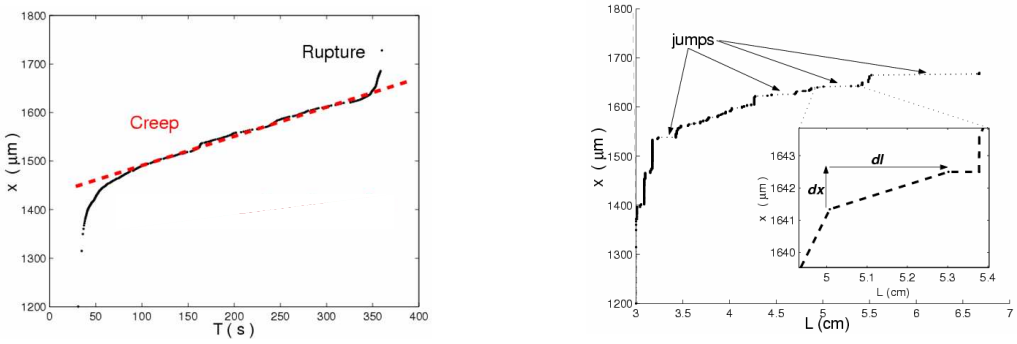

Figure 10: a) Deformation of a sheet of paper with an initial defect of $L_i = 3$cm during an experiment at a constant load $F = 190$N. b) Deformation of the sheet of paper as function of the crack length for the same experiment.

that the work developed by the tensile machine will only permit the crack to advance (we neglect any source of dissipation), we can estimate an upper bound for the surface energy γ. Indeed the minimum work provided by the tensile machine when making a displacement dx at a constant load F in order to open the crack of a length dl is $\delta W_{min} = Fdx = 4\gamma edl$. Therefore we can give an upper limit for the surface energy : $\gamma = Fdx/4edl$, when the crack advances of dl for a displacement dx of the tensile machine, where e is the width of the sheet submitted to a constant force F.

However, during a creep experiment, we observe a slow global deformation of the sheet of paper (see fig.10a) which is uncorrelated with the crack growth. In order to suppress this creep effect that will lead to an over-estimation of the surface energy γ we will examine the displacement of the tensile machine dx when the crack advances by jumps (see fig.10b)) which occurs over much faster temporal scales than the creep deformation. We can repeat this analysis for the various jumps detected during the slow crack growth and finally for the various experiments performed. Therefore, we obtain an average value for the surface energy $\langle\gamma\rangle = 1540 \pm 180$N/m (Note that the dispersion of this measurement is really important, $\langle\gamma^2\rangle^{1/2} = 850$N/m).

With this measurement of the surface energy we get an estimate of the average Griffith length $\langle L_G\rangle$, using the Young modulus of the fax paper sheets $Y = 3.3\,10^9$N.m^{-2}, and finally we compare this length to the critical length measured during our creep experiments where the paper sheet breaks suddenly. Fig.11a) shows the average critical length $\langle L_c\rangle$ as a function of the

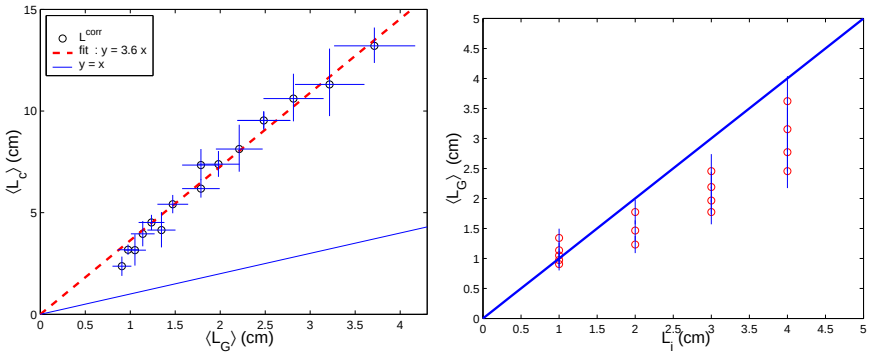

Figure 11: a) Average critical length $\langle L_c \rangle$ as function of the Griffith $\langle L_G \rangle$. The dashed line represents the best linear fit $y = 3.6x$ while the continuous line is a guide for the eye showing $y = x$. b) Average Griffith length $\langle L_G \rangle$ as function of the initial crack length L_i. The line $y = x$ is a guide for the eye.

average Griffith length $\langle L_G \rangle$ for the various creep experiments performed. We observe clearly that the critical length for rupture is at least 3 times larger that the critical length predicted by Griffith. Moreover it is important to recall that we actually estimated an upper limit of this Griffith length since the slow deformation of the sample during the creep experiments leads to an over-estimation of the surface energy needed to open a crack which was also by definition an upper bound of the surface energy of our samples. Thus, we could expect the Griffith length to be even smaller. We can also notice on fig.11b) that the Griffith length is for all the various experiments performed smaller or very close to the initial crack length L_i. This suggests that L_G might be indeed a critical length below which no crack propagation can occur, at least during a reasonable experimental time.

3.2.4 Comparison with the model describing the statistically averaged crack growth

The experimental measurements of the mean crack growth in paper sheets show a rather good agreement with the predictions of the activation model described in 2. Indeed the model predicts the evolution of the crack length as a function of time, the characteristic length ζ and the life time τ of the sample as a function of the applied stress and the temperature. It is important to notice that the only free adjustable parameter is the activation volume V which represents the scale at which the statistical stress fluctuations trigger rupture events. This activation volume V turns out to be about the same, within error bars, in the fits of two very different measured physical quantities τ and ζ as a function of the theoretical predictions. It is an interesting experimental evidence that $V^{1/3}$ is extremely close to the diameter d of the microfibrils that make up the macroscopic paper fibers [27], suggesting that the rupture first occurs inside a fiber at the nanometric scale of the microfibrils and then progressively leads to the rupture of the paper fiber itself. It is possible to include such a progressive rupture mechanism of the macroscopic fiber in the rupture model that we discuss in this paper. Indeed, the rupture time of a bundle of micofibrils is dominated by the same exponential factor than the one used for τ_V in equation (6). It was argued in [31] that the volume at which rupture occurs is then $V = d^3$ while the stress level in the microfibrils is set by the whole bundle

diameter $\lambda \simeq \sqrt{n}d$, where n is the number of microfibrils making up the macroscopic fiber. It is rather commonly observed that the subcritical time of rupture is controlled by thermally activated mechanisms at the nanometer scale [4, 32]. In addition to connecting this nanometer scale to a microstructure of the material, we show that it is also possible to describe the whole growth dynamics in a brittle material using the ambient temperature for T, without having to take into account an effect of disorder through an effective temperature [10].

Moreover, we show that, in our creep experiments, the Griffith critical length L_G corresponding to the maximum of the Griffith potential energy is smaller than the critical length of rupture L_C as well as the initial crack length L_i. This result is in agreement with previous predictions [21], and with our numerical simulations on a 2D elastic spring network. It also appears consistent with the picture described in section 2.3 where, due to the lattice trapping, a crack with a length above the Griffith length will grow irreversibly even if one assumes that the rupture is reversible.

4 Statistics of the jumps of the crack tip

Looking at the typical growth curve plotted in Fig.6a) it clearly appears that the crack does not grow smoothly: essentially, there are periods of rest where the crack tip does not move and periods where it suddenly opens and advances of a certain step size s. In sect.3 we have seen that varying the initial crack length ($1cm < L_i < 4cm$) and the initial stress intensity factor K_i between 2.7MPa.m$^{1/2}$ and 4.2MPa.m$^{1/2}$, the resulting measured lifetime varied from a few seconds to a few days depending on the value of the applied stress or the temperature. Even for the same experimental conditions (same stress, initial crack length and temperature) a strong dispersion in lifetime is observed. This is of course expected for a model of thermally activated growth [11] as the one discussed in sect.2 which describes the mean behavior of the crack, as we have shown in sect.3. Here, we want to study more extensively the step size statistics and to check if our model may describe the distributions of the jump amplitudes.

4.1 Experimental results

In sect.3 we have seen that the crack velocity is an increasing function of the stress intensity factor K. Thus, it is natural to look at the step statistics for a given value of K. We have seen also that the $p(s)$ predicted by our model (eq.13) is a function of K. In practice, the step size distributions have been obtained for various ranges of K.

Fig.12a) shows the step size distributions determined from all the data we have collected using a logarithmic binning. Typically, 700 data points are used to obtain each distribution. Two regimes are observed. For small step sizes, the distribution does not depend on the value of K, while for larger step sizes there is a cut-off size increasing with K. In practice, the toughness of the material, i.e. its critical stress intensity factor $K_c = 6.5 \pm 0.05$MPa.m$^{1/2}$, has been obtained as the value of K beyond which the probability to detect a jump vanishes.

The normalization condition of the distribution actually reduces the model to one parameter, the ratio V/λ^2. As we have already done in sect.3 we fix $\lambda = 50\mu$m and V is the only unknown. Using for $p(s)$ the expression derived in eq.13, one parameter fits of step size distributions in Fig.12a) for each range of stress intensity factors give very robust results. We find $V = 5 \pm 1$ Å^3 which is quite different from the value obtained from the fits of the average dynamics in sect.3. The possible reasons of this difference will be discussed in the next section. Here we focus on the comparison between the computed $p(s)$ eq.13 and the measured one. To check the asymptotic limit close to the critical point, we have plotted in Fig.12 $\langle s \rangle$ and $\langle s^2 \rangle^{1/3}$ as a function of $K_c/(K_c - K_m)$. Here, the mean and the variance of step sizes

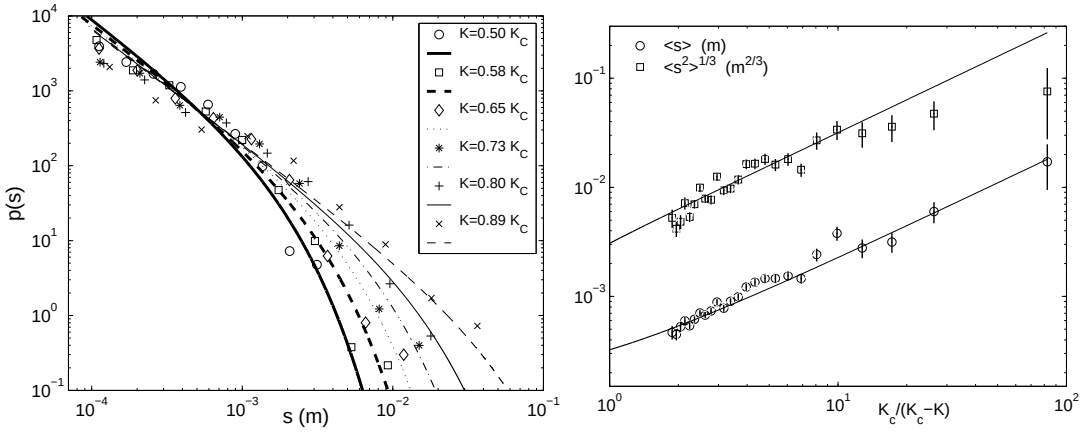

Figure 12: a) Probability distribution of step sizes for various values of stress intensity factor. Choosing $\lambda = 50\mu$m, the different curves are the best fits of eq.13 giving an average value $V = (5\pm1)$ Å^3. b)The mean and cubic root of the variance from raw measurements of step sizes is well reproduced by the model (eq.(14) and eq.(15)) plotted with $\lambda = 50\mu$m and $V = 5$ Å^3.

have been computed from the raw measurements in a given range of K. Because it requires less statistics to estimate the first two moments of the distribution than the distribution itself, we are able to narrow the width of the K range for each data point without changing the global trend. The solid lines represents the model prediction using the fitted value of V from the distributions of Fig.12. Not only the model reproduces reasonably well the evolution of the step size distributions with K (V is essentially constant and all the other parameters are fixed), but the asymptotic divergence of the first two moments of the distribution are also well reproduced. For the mean step size, the scaling is observed up to K values very close to K_c, about 1%. In the model, we see that the ratio of the standard deviation of the distribution over the mean size is diverging at K_c. Thus, close to K_c, the measure of variance becomes more inaccurate than for the mean.

4.2 Limits of this approach

We note that some experimental observations are not taken into account by our model. For instance, it could have been expected from [9] that the distribution of waiting times should be exponential. On Fig.13, we see that the distribution is not exponential. As a guide for the eye, we show that for small times the slope in log-log scale is around 2/3 and for larger times 2. Also, the model does not consider the roughness that the crack develops and the effect it has on the local stress field. This will change the dynamics of the crack growth and it would be interesting to make a connection with the statistical properties of the crack roughness discussed in [30, 31, 33].

More important, we have noticed in the previous section that the value of V obtained from the fit of the measured $p(s)$ is at the atomic scale, i.e. $V^{1/3} \simeq 1.7$ Å. This scale is one order of magnitude below the one obtained from the fits of the average dynamics in sect.3. There are several reasons for this difference. It should be realized that the model for the jumps actually predicts a lower limit for this microscopic scale. Indeed $s \propto U_f \lambda / U_c$ is a simple dimensional argument and the prefactor is unknown. We arbitrarily fixed it to 1, but this prefactor could be

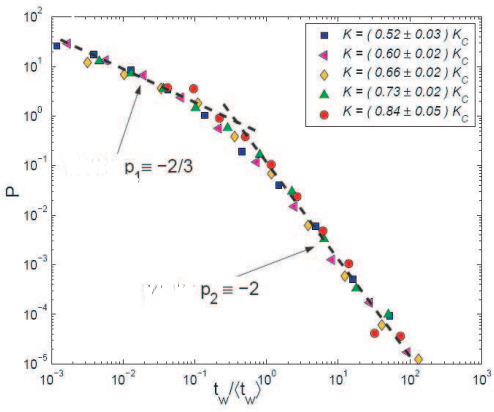

Figure 13: Distribution of waiting times between two crack jumps. All the distributions for various ranges of stress intensity factor collapse on a single curve when normalized by the average waiting time value corresponding to each range.

much larger. Our choice implicitly assumes that there is a strong dissipation of energy during crack advance since none of the elastic release of energy is used to keep the crack moving, This is certainly an overestimation of a real dissipative mechanism, would it be viscoelastic or plastic. Decreasing dissipation in the model will permit larger steps of the crack. In order to obtain the same experimental velocity, the trapping time must also be larger which will happen if the rupture occurs at a larger microscopic scale. The other point that has been neglected is the disorder in the material properties. It has been shown recently that disorder effectively reduce the energy cost for breaking and this will also permit rupture at a larger microscopic scale [10]. However, several recent works have shown that when a macroscopic crack is growing, the disorder will actually help pin the crack and slows down its dynamic [28, 29]. Thus, further theoretical work needs to be done mainly with the aim of introducing a more realistic dissipative mechanism.

Despite these limitations, we believe that our approach in the present form is a first step to describe rupture in brittle materials for which a structure at a mesoscopic scale exists. At this point, the rupture model presented in this paper can not describe rupture in ductile materials and we expect that taking into account plasticity, for instance, will lead to significantly different growth dynamics [34].

5 Conclusion

To conclude, we have seen that the slow crack dynamics in fibrous materials such as paper is a complex and rich statistical process. Specifically, we have studied the sub-critical growth of a single crack during creep experiments and observed stepwise growth dynamics. Despite this complexity, a statistical average of the growth dynamics reveals a simple behavior. We have shown that a simple model of irreversible and thermally activated rupture is able to predict with good accuracy the average crack growth observed, which can be characterized by only two parameters: the rupture time τ and a characteristic growth length ζ. Both quantities are in reasonable agreement with the model. In particular, we verified experimentally that rupture time depends exponentially on temperature as previously observed [4]. The comparison of our

experimental results on the averaged crack growth to the thermally activated rupture model suggests that the thermodynamical stress fluctuations have a proper amplitude to trigger rupture events at a nanometric scale corresponding to the width of cellulose microfibrils. This is consistently found from two independent measurements : the rupture time τ and a characteristic growth length ζ.

Moreover, we have shown [25] that we can adapt and extend our first model [11] in order to describe the stepwise growth dynamics in a rugged potential energy landscape. The microstructure of our samples could indeed modify the Griffith energy barrier leading to a lattice trapping effect [22]). As a consequence this modified model predicts the step size statistics. This is quite interesting because it may open new perspectives in the description of rupture as a thermally activated process. However concerning this last approach more work is needed to introduce a more realistic dissipative mechanism in the material properties in order to understand the reasons why the activation volume obtained from the jump statistics (section 4) is smaller than the volume obtained obtained from the average crack growth properties in (section 3).

Acknowledgements This paper is dedicated to the memory of Carlos Perez Garcia. One of us (S.C.) remembers him not only for the very interesting scientific collaborations and useful discussions but mainly for his kindness and warm friendship.

References

[1] H. J. Herrmann, S. Roux, *Statistical models for the fracture of disordered media* (Elsevier, Amsterdam, 1990).

[2] M. J. Alava, P. K. N. N. Nukala, S. Zapperi, Adv. in Phys. **55**, 349-476 (2006).

[3] S. S. Brenner, J. Appl. Phys. **33**, 33 (1962).

[4] S. N. Zhurkov, Int. J. Fract. Mech. **1**, 311 (1965).

[5] L. Golubovic, S. Feng, Phys. Rev. A **43**, 5223 (1991).

[6] Y. Pomeau, C.R. Acad. Sci. Paris II **314** 553 (1992); C.R. Mécanique **330**, 1 (2002).

[7] A. Buchel, J. P. Sethna, Phys. Rev. Lett. **77**, 1520 (1996); Phys. Rev. E **55**, 7669 (1997).

[8] K. Kitamura I. L. Maksimov, K. Nishioka, Phil. Mag. Lett. **75**, 343 (1997).

[9] S. Roux, Phys. Rev. E **62**, 6164 (2000).

[10] R. Scorretti, S. Ciliberto, A. Guarino, Europhys. Lett. **55**(5), 626 (2001);

[11] S. Santucci, L. Vanel, R. Scorretti, A. Guarino, S. Ciliberto, Europhys. Lett. **62**, 320 (2003).

[12] R. A. Schapery, *In Encyclopedia of Material Science and Engineering* (Pergamon, Oxford, 1986), p. 5043.

[13] J. S. Langer, Phys. Rev. Lett. **70**, 3592 (1993).

[14] A. Chudnovsky, Y. Shulkin, Int. J. of Fract. **97**, 83 (1999).

[15] P. Paris, F. Erdogan, J. Basic Eng., **89**, 528 (1963).

[16] A. A. Griffith, Phil. Trans. Roy. Soc. Lond. A **221**, 163 (1920).

[17] B. Lawn , T. Wilshaw, *Fracture of Brittle Solids* (Cambridge University Press, Cambridge, 1975).

[18] L. Pauchard, J. Meunier, Phys. Rev. Lett. **70**, 3565 (1993).

[19] S. Ciliberto, A. Guarino, R. Scorretti, Physica D **158**, 83 (2001).

[20] B. Diu , C. Guthmann, D. Lederer, B. Roulet, *Physique Statistique* (Herrmann, Paris 1989), 272.

[21] M. Marder, Phys. Rev. E **54**, 3442 (1996).

[22] R. Thomson, in *Solid State Physics*, edited by H. Ehrenreich and D. Turnbull (Academic, New York, 1986), Vol. 39, p. 1.

[23] D. Stauffer, *Introduction to Percolation Theory* (Taylor & Francis, London, 1991).

[24] S. Santucci, P-P. Cortet, S. Deschanel, L. Vanel, S. Ciliberto, Europhys. Lett. **74** (4), 595 (2006).

[25] S. Santucci, L. Vanel, S. Ciliberto, Phys. Rev. Lett. **93**, 095505 (2004).

[26] A. Guarino, S. Ciliberto, A. Garcimartìn, Europhys. Lett. **47** (4), 456 (1999).

[27] H. F. Jakob, S. E. Tschegg, P. Fratzl, J. Struct. Biol. **113**, 13 (1994).

[28] P.-P. Cortet, L. Vanel, S. Ciliberto, Europhys. Lett. **74**, 602 (2006).

[29] J. Kierfeld, V. M. Vinokur, Phys. Rev. Lett. **96**, 175502 (2006).

[30] E. Bouchbinder, I. Procaccia, S. Santucci, L. Vanel, Phys. Rev. Lett. **96**, 055509 (2006).

[31] S. Santucci, K. J. Måloy, A. Delaplace, J. Mathiesen, A. Hansen, J. O. Haavig Bakke, J. Schmittbuhl, L. Vanel, P. Ray, Phys. Rev. E., **75** 016104 (2007).

[32] F. Bueche, J. App. Phys. **28**(7), 784 (1957).

[33] N. Mallick, P-P. Cortet, S. Santucci, S. Roux, L. Vanel. submitted. to Phys. Rev. Lett. (2006).

[34] P.P. Cortet, S. Santucci, L.Vanel, S. Ciliberto, Europhys. Lett. **71** (2), 1 (2005).